# Linear-scaling implementation of molecular response theory in self-consistent field electronic-structure theory

Sonia Coriani
*Dipartimento di Scienze Chimiche, Università degli Studi di Trieste, Via Licio Giorgieri 1, I-34127 Trieste, Italy*

Stinne Høst,[a] Branislav Jansík, Lea Thøgersen, Jeppe Olsen, and Poul Jørgensen
*The Lundbeck Foundation Center for Theoretical Chemistry, Department of Chemistry, University of Aarhus, DK-8000 Århus C, Denmark*

Simen Reine,[b] Filip Pawłowski,[c] and Trygve Helgaker[d]
*Centre of Theoretical and Computational Chemistry, Department of Chemistry, University of Oslo, P.O. Box 1033 Blindern, N-0315 Norway*

Paweł Sałek
*Department of Theoretical Chemistry, The Royal Institute of Technology, SE-10691 Stockholm, Sweden*

(Received 1 November 2006; accepted 15 February 2007; published online 18 April 2007)

A linear-scaling implementation of Hartree-Fock and Kohn-Sham self-consistent field theories for the calculation of frequency-dependent molecular response properties and excitation energies is presented, based on a nonredundant exponential parametrization of the one-electron density matrix in the atomic-orbital basis, avoiding the use of canonical orbitals. The response equations are solved iteratively, by an atomic-orbital subspace method equivalent to that of molecular-orbital theory. Important features of the subspace method are the use of paired trial vectors (to preserve the algebraic structure of the response equations), a nondiagonal preconditioner (for rapid convergence), and the generation of good initial guesses (for robust solution). As a result, the performance of the iterative method is the same as in canonical molecular-orbital theory, with five to ten iterations needed for convergence. As in traditional direct Hartree-Fock and Kohn-Sham theories, the calculations are dominated by the construction of the effective Fock/Kohn-Sham matrix, once in each iteration. Linear complexity is achieved by using sparse-matrix algebra, as illustrated in calculations of excitation energies and frequency-dependent polarizabilities of polyalanine peptides containing up to 1400 atoms. © *2007 American Institute of Physics*. [DOI: 10.1063/1.2715568]

## I. INTRODUCTION

Quantum chemistry has evolved in a spectacular fashion during the last two decades. Using quantum-chemical methods, it is nowadays possible to investigate a large number of molecular properties of increasing complexity, from computationally simple energy differences such as reaction enthalpies to more involved high-order frequency-dependent polarizabilities and multiphoton strengths, with control over the accuracy of the results.[1] Molecular properties are fundamental quantities underlying the macroscopic behavior of matter and their determination constitutes one of the most fruitful areas of interplay between experiment and theory.[2]

A difficulty in the application of quantum chemistry to compute molecular properties is the restriction on the size of systems that can be treated by current technology. Even with the recent dramatic improvements in computer technology and introduction of Kohn-Sham theory, the routine study of systems such as myoglobin, containing 150 amino acids, is still beyond our capabilities. This situation is particularly unfortunate in view of the considerable academic and industrial interest in macromolecules containing thousands of atoms such as polymers, proteins, enzymes, and nucleic acids.

The bottleneck for quantum-mechanical methods in their application to large systems is the scaling of the cost—in other words, the increase of CPU usage with increasing system size. Formally, Hartree-Fock and Kohn-Sham self-consistent field (SCF) methods scale as $O(N^4)$, where $N$ refers to the system size. Moreover, wave-function-based correlated methods typically scale as $O(N^5)$ or higher. With such a steep scaling, advances in computer hardware alone will never allow us to treat large systems such as myoglobin. During the last decade, a large effort has been directed towards the development of new algorithms with a better scaling—see, for instance, Refs. 3–5 and references therein. The goal is to develop "linear-scaling" methods—that is, methods where the computational cost scales linearly with the system size, $O(N)$.

In Hartree-Fock and Kohn-Sham theories, the two major obstacles for the optimization of the energy have now been eliminated—namely, the construction of the Fock/Kohn-

[a]Author to whom correspondence should be addressed. Electronic mail: stinne@chem.au.dk
[b]Present address: Department of Chemistry, University of Aarhus, DK-8000 Århus C, Denmark.
[c]Present address: Institute of Physics, Kazimierz Wielki University, Plac Weyssenhoffa 11, 85-072 Bydgoszcz, Poland.
[d]Present address: Department of Chemistry, University of Durham, South Road, Durham DH1 3LE, UK.

 

Sham (KS) matrix and the generation of a new density matrix from the current Fock/KS matrix, see Ref. 3 for a recent overview. With these obstacles removed, it has become appropriate to address the problem of calculating molecular properties at linear cost.

In this paper, we describe a linear-scaling method for the calculation of molecular properties that may be expressed in terms of frequency-dependent response functions and their poles and residues. In particular, we consider properties calculated from the linear response function such as frequency-dependent polarizabilities, excitation energies, and one-photon transition moments. Molecular properties that are expressed in terms of higher-order response functions[6] can be obtained by a straightforward extension of the presented scheme.

In our linear-scaling response implementation, the expressions for the response functions are derived using a non-redundant exponential parametrization of the density matrix in the atomic-orbital (AO) basis. The formal derivation of the response functions and their residues is given in Refs. 7–9; for perturbation-dependent basis sets (used to calculate geometrical derivatives with atom-fixed AOs and magnetic properties with London AOs), the theory is given in Ref. 8. In this paper, we only discuss computational aspects that exclusively refer to property calculations; the strategy adopted for linear-scaling energy optimizations is described in Ref. 3.

Since all key computational steps of response theory presented here consist of multiplications of density, Fock/KS, and property matrices in the AO basis, matrix sparsity must be explored to achieve linear scaling. First, the response eigenvalue equations and linear sets of equations are solved. Their solution constitutes the major challenge with respect to linear scaling. We describe here how this may be achieved with iterative AO techniques, generalizing the algorithm previously developed to solve the response equations in the molecular-orbital (MO) basis at various levels of theory.[10,11]

An important feature of the response solver is that it maintains the paired structure of the response generalized Hessian and metric matrices. By adding trial vectors in pairs, the solver imposes the paired structure of the full-space response equations on the reduced-space equations, ensuring that complex eigenvalues do not arise during their solution. Furthermore, monotonic convergence is ensured towards the lowest eigenvalues. Another important feature of our algorithm is that we take over, in the AO basis, the preconditioner that has been so successfully employed in the MO basis. However, this preconditioner cannot be applied directly in the AO basis as the generalized AO Hessian has a large condition number and is not diagonally dominant. Rather, it is applied in an orthogonalized AO basis such as those defined by the Cholesky or Löwdin symmetric decomposition of the overlap matrix. In such a basis, the generalized Hessian becomes diagonally dominant and the condition number is significantly reduced. For the optimization of Hartree-Fock and Kohn-Sham energies, the Newton equations have previously been successfully solved when transformed from the AO basis to the Löwdin basis[3] or the Cholesky basis.[12]

The evaluation of static molecular properties within a linear-scaling framework has previously been considered by Ochsenfeld and Head-Gordon,[13] adopting a parametrization of the density matrix where idempotency is taken care of by replacing the density matrix with its McWeeny-purified counterpart,[14] as suggested by Li *et al.*[15] Using this approach, Ochsenfeld *et al.* have reported a linear-scaling implementation of NMR shifts for linear alkanes and presented results for three-dimensional systems with more than 1000 atoms.[16] An alternative strategy for static molecular properties, based on a purification of the density matrix, has recently been proposed by Weber *et al.*[17]

The remainder of this paper is divided into three main sections. In Sec. II, we present the theory and implementation of linear-scaling SCF linear response theory. Section III contains some numerical examples of calculations of frequency-dependent polarizabilities and excitation energies. Finally, Sec. IV contains some concluding remarks.

## II. THEORY

The present section consists of four parts. First, in Sec. II A, the basic expressions of AO-based linear response theory are given, in a manner suitable for linear-scaling implementation. In Sec. II B we discuss the iterative algorithm used for solving the response equations. Finally, in Secs. II C and II D, respectively, we describe preconditioning and initial guesses of the iterative algorithm.

### A. AO-based SCF linear response theory

In Hartree-Fock and Kohn-Sham theories, response functions may be efficiently calculated in the AO basis, expressing the AO density matrix in the exponential form[1,7,18–21]

$$\mathbf{D}(\mathbf{X}) = \exp(-\mathbf{XS})\mathbf{D}\exp(\mathbf{SX}), \tag{1}$$

where $\mathbf{S}$ is the AO overlap matrix and $\mathbf{X}$ is an anti-Hermitian matrix that contains the variational parameters, with the redundant parameters projected out:

$$\mathbf{X} = \mathcal{P}(\mathbf{X}). \tag{2}$$

We have here introduced the projection operator on a matrix $\mathbf{M}$,

$$\mathcal{P}(\mathbf{M}) = \mathbf{P}_o\mathbf{M}\mathbf{P}_v^T + \mathbf{P}_v\mathbf{M}\mathbf{P}_o^T, \tag{3}$$

where $\mathbf{P}_o$ and $\mathbf{P}_v$ are projectors onto the occupied and virtual orbital spaces, respectively,

$$\mathbf{P}_o = \mathbf{DS}, \tag{4}$$

$$\mathbf{P}_v = \mathbf{I} - \mathbf{DS}, \tag{5}$$

fulfilling the idempotency ($\mathbf{P}_o^2=\mathbf{P}_o$ and $\mathbf{P}_v^2=\mathbf{P}_v$) and orthogonality relations ($\mathbf{P}_o\mathbf{P}_v=\mathbf{P}_v\mathbf{P}_o=\mathbf{0}$ and $\mathbf{P}_o^T\mathbf{S}\mathbf{P}_v=\mathbf{P}_v^T\mathbf{S}\mathbf{P}_o=\mathbf{0}$). Using the above exponential parametrization of the AO density matrix, the linear response function associated with the time-independent operators $\hat{A}$ and $\hat{B}$ becomes[7]

$$\langle\langle \hat{A};\hat{B}\rangle\rangle_\omega = \mathrm{Tr}[\mathbf{A}^{[1]}\mathbf{N}^B(\omega)], \tag{6}$$

$$(\mathbf{E}^{[2]} - \omega\mathbf{S}^{[2]})\text{vec}\,\mathbf{N}^{B}(\omega) = -\,\text{vec}\,\mathbf{B}^{[1]}, \tag{7}$$

where $\mathbf{M}^{[1]}$ is the property gradient of the operator $\hat{M}$ represented by the AO matrix $\mathbf{M}$:[7]

$$\mathbf{M}^{[1]} = \mathbf{SDM} - \mathbf{MDS} = \mathbf{P}_{\mathrm{o}}^{\mathrm{T}}\mathbf{M} - \mathbf{MP}_{\mathrm{o}}. \tag{8}$$

In Eq. (7), the vec operator transforms a matrix $\mathbf{M}$ into a column vector vec $\mathbf{M}$ by stacking its columns. Since the linear equations are solved iteratively, the generalized Hessian matrix $\mathbf{E}^{[2]}$ and the metric matrix $\mathbf{S}^{[2]}$ are not needed explicitly but may instead be defined in terms of their linear transformations of an arbitrary trial vector vec $\mathbf{b}$. Thus, in the notations

$$\text{vec}\,\mathbf{E}^{[2]}(\mathbf{b}) = \mathbf{E}^{[2]}\,\text{vec}\,\mathbf{b}, \tag{9}$$

$$\text{vec}\,\mathbf{S}^{[2]}(\mathbf{b}) = \mathbf{S}^{[2]}\,\text{vec}\,\mathbf{b}, \tag{10}$$

the Hessian and metric linear transformations are given by[7]

$$\boldsymbol{\sigma} = \mathbf{E}^{[2]}(\mathbf{b}) = \mathcal{P}_{\mathrm{T}}[\mathbf{FD}_{\mathrm{b}}\mathbf{S} - \mathbf{SD}_{\mathrm{b}}\mathbf{F} + \mathbf{G}(\mathbf{D}_{\mathrm{b}})\mathbf{DS} - \mathbf{SDG}(\mathbf{D}_{\mathrm{b}})], \tag{11}$$

$$\boldsymbol{\rho} = \mathbf{S}^{[2]}(\mathbf{b}) = -\,\mathcal{P}_{\mathrm{T}}(\mathbf{SD}_{\mathrm{b}}\mathbf{S}). \tag{12}$$

Here the Fock/KS matrix takes the form

$$\mathbf{F} = \mathbf{h} + \mathbf{G}(\mathbf{D}), \tag{13}$$

where $\mathbf{G}(\mathbf{D})$ denotes the Coulomb and exact-exchange contributions. In Kohn-Sham theory, there is an additional contribution from the exchange-correlation potential, not included here. All formulas, however, are equally valid for Kohn-Sham theory. We have furthermore introduced the projector

$$\mathcal{P}_{\mathrm{T}}(\mathbf{M}) = \mathbf{P}_{\mathrm{o}}^{\mathrm{T}}\mathbf{MP}_{\mathrm{v}} + \mathbf{P}_{\mathrm{v}}^{\mathrm{T}}\mathbf{MP}_{\mathrm{o}} \tag{14}$$

by analogy with Eq. (3) and the transformed density matrix

$$\mathbf{D}_{\mathrm{b}} = [\mathcal{P}(\mathbf{b}),\mathbf{D}]_{\mathrm{S}} = \mathcal{P}([\mathbf{b},\mathbf{D}]_{\mathrm{S}}) = \mathbf{P}_{\mathrm{v}}\mathbf{bP}_{\mathrm{o}}^{\mathrm{T}} - \mathbf{P}_{\mathrm{o}}\mathbf{bP}_{\mathrm{v}}^{\mathrm{T}} \tag{15}$$

in terms of the S commutator $[\mathbf{M},\mathbf{N}]_{\mathrm{S}} = \mathbf{MSN} - \mathbf{NSM}$. Assuming that $\mathcal{P}(\mathbf{b}) = \mathbf{b}$, we may also write the linear transformations Eqs. (11) and (12) in the form

$$\mathbf{E}^{[2]}(\mathbf{b}) = (\mathbf{F}^{\mathrm{vv}} - \mathbf{F}^{\mathrm{oo}})\mathbf{bS} + \mathbf{Sb}(\mathbf{F}^{\mathrm{vv}} - \mathbf{F}^{\mathrm{oo}}) + \mathbf{G}^{\mathrm{vo}}(\mathbf{D}_{\mathrm{b}}) - \mathbf{G}^{\mathrm{ov}}(\mathbf{D}_{\mathrm{b}}), \tag{16}$$

$$\mathbf{S}^{[2]}(\mathbf{b}) = -\,\mathbf{S}^{\mathrm{vv}}\mathbf{bS}^{\mathrm{oo}} + \mathbf{S}^{\mathrm{oo}}\mathbf{bS}^{\mathrm{vv}}, \tag{17}$$

where we have introduced the notation

$$\mathbf{M}^{\mathrm{mn}} = \mathbf{P}_{\mathrm{m}}^{\mathrm{T}}\mathbf{MP}_{\mathrm{n}}, \tag{18}$$

noting that $\mathbf{S}^{\mathrm{vo}} = \mathbf{S}^{\mathrm{ov}} = \mathbf{0}$.

Excitation energies—that is, the poles of the linear response function in Eq. (6)—are the eigenvalues of the generalized eigenvalue problem

$$(\mathbf{E}^{[2]} - \omega_{n0}\mathbf{S}^{[2]})\text{vec}\,\mathbf{X}_n = \mathbf{0}, \tag{19}$$

where $\omega_{n0}$ is the excitation energy from the ground state $|0\rangle$ to the excited state $|n\rangle$. The corresponding transition moment of $\hat{A}$ is obtained from the residue of the linear response function

$$\langle 0|\hat{A}|n\rangle = \mathrm{Tr}[\mathbf{A}^{[1]}\mathbf{X}_n]. \tag{20}$$

In this paper, we describe how linear response functions, excitation energies, and transition moments (one-photon transition strengths) may be evaluated at a cost that, for sufficiently large systems, scales linearly with system size.

In iterative algorithms, which are here used to solve the response equations, the Hessian and metric linear transformations Eqs. (11) and (12) require the AO overlap matrix $\mathbf{S}$, the AO density matrix $\mathbf{D}$, and the AO Fock/KS matrix $\mathbf{F}$, all of which are also needed for the (linear-scaling) AO-based optimization of the energy.[3] The additional contribution from $\mathbf{G}(\mathbf{D}_{\mathrm{b}})$ in Eq. (11), which is not needed for energy optimizations, can also be calculated at linear cost. The transformations Eqs. (11) and (12) consist entirely of sparse-matrix algebra and may for sufficiently large systems be carried out in linear time. We now turn our attention to the linear-scaling iterative solution of the linear set of equations Eq. (7) and the eigenvalue problem Eq. (19). Once their solutions have been found, molecular properties are straightforwardly obtained as the trace of sparse matrices Eqs. (6) and (20).

### B. Iterative solution of response equations

Before describing the iterative algorithm, we note the relations

$$[\mathbf{E}^{[2]}(\mathbf{b})]^{\mathrm{T}} = \mathbf{E}^{[2]}(\mathbf{b}^{\mathrm{T}}), \tag{21}$$

$$[\mathbf{S}^{[2]}(\mathbf{b})]^{\mathrm{T}} = -\,\mathbf{S}^{[2]}(\mathbf{b}^{\mathrm{T}}). \tag{22}$$

Therefore, if the transformations Eqs. (11) and (12) are known for a given trial matrix $\mathbf{b}_i$,

$$\boldsymbol{\sigma}_i = \mathbf{E}^{[2]}(\mathbf{b}_i), \tag{23}$$

$$\boldsymbol{\rho}_i = \mathbf{S}^{[2]}(\mathbf{b}_i), \tag{24}$$

they are also known for the transposed trial matrix,

$$\boldsymbol{\sigma}_i^{\mathrm{T}} = \mathbf{E}^{[2]}(\mathbf{b}_i^{\mathrm{T}}), \tag{25}$$

$$-\,\boldsymbol{\rho}_i^{\mathrm{T}} = \mathbf{S}^{[2]}(\mathbf{b}_i^{\mathrm{T}}). \tag{26}$$

Since the transformations of $\mathbf{b}_i$ and $\mathbf{b}_i^{\mathrm{T}}$ are related to each other in such a simple manner, new trial matrices are always added in pairs $\mathbf{b}_i$ and $\mathbf{b}_i^{\mathrm{T}}$.

Let us now assume that we solve the response equations Eq. (7) iteratively and that, in the course of the iterations, $n$ pairs of trial matrices have been generated. These matrices constitute a $2n$-dimensional reduced basis:

$$\mathbf{b}^{2n} = \{\mathbf{b}_1,\mathbf{b}_1^{\mathrm{T}},\mathbf{b}_2,\mathbf{b}_2^{\mathrm{T}},\ldots,\mathbf{b}_n,\mathbf{b}_n^{\mathrm{T}}\}. \tag{27}$$

We assume that the trial matrices are orthonormal,

$$\mathrm{Tr}(\mathbf{b}_i\mathbf{b}_j) = \mathrm{Tr}(\mathbf{b}_i^{\mathrm{T}}\mathbf{b}_j^{\mathrm{T}}) = \delta_{ij}, \tag{28}$$

$$\mathrm{Tr}(\mathbf{b}_i^{\mathrm{T}}\mathbf{b}_j) = \mathrm{Tr}(\mathbf{b}_i\mathbf{b}_j^{\mathrm{T}}) = 0, \tag{29}$$

and that they satisfy the projection relation

$$\mathbf{b}_i = \mathcal{P}(\mathbf{b}_i). \tag{30}$$

The transformed trial matrices $\boldsymbol{\sigma}_i = \mathbf{E}^{[2]}(\mathbf{b}_i)$ and $\boldsymbol{\rho}_i = \mathbf{S}^{[2]}(\mathbf{b}_i)$ are then given by

$$\boldsymbol{\sigma}^{2n} = \{\boldsymbol{\sigma}_1, \boldsymbol{\sigma}_1^{\mathrm{T}}, \boldsymbol{\sigma}_2, \boldsymbol{\sigma}_2^{\mathrm{T}}, \ldots, \boldsymbol{\sigma}_n, \boldsymbol{\sigma}_n^{\mathrm{T}}\}, \tag{31}$$

$$\boldsymbol{\rho}^{2n} = \{\boldsymbol{\rho}_1, -\boldsymbol{\rho}_1^{\mathrm{T}}, \boldsymbol{\rho}_2, -\boldsymbol{\rho}_2^{\mathrm{T}}, \ldots, \boldsymbol{\rho}_n, -\boldsymbol{\rho}_n^{\mathrm{T}}\}. \tag{32}$$

The basis of trial matrices and their transformed counterparts are then used to set up the response equations in a reduced space of dimension $2n$:

$$(\mathbf{E}_{\mathrm{R}}^{[2]} - \omega \mathbf{S}_{\mathrm{R}}^{[2]})\mathbf{X}_{\mathrm{R}} = -\mathbf{B}_{\mathrm{R}}^{[1]}, \tag{33}$$

where the reduced-space gradient elements are given as

$$(\mathbf{B}_{\mathrm{R}}^{[1]})_i = \mathrm{Tr}[(\mathbf{B}^{[1]})^{\mathrm{T}} \mathbf{b}_i^{2n}], \tag{34}$$

whereas the reduced-space generalized Hessian and metric matrices become

$$(\mathbf{E}_{\mathrm{R}}^{[2]})_{ij} = \mathrm{Tr}[(\mathbf{b}_i^{2n})^{\mathrm{T}} \boldsymbol{\sigma}_j^{2n}], \tag{35}$$

$$(\mathbf{S}_{\mathrm{R}}^{[2]})_{ij} = \mathrm{Tr}[(\mathbf{b}_i^{2n})^{\mathrm{T}} \boldsymbol{\rho}_j^{2n}]. \tag{36}$$

The reduced equations Eq. (33) are easily solved since the dimension $2n$ is small.

From the solution to the reduced problem Eq. (33), we may expand the current optimal solution matrix $\mathbf{X}$ as

$$\mathbf{X} = \sum_{i=1}^{2n} (X_{\mathrm{R}})_i \mathbf{b}_i^{2n}, \tag{37}$$

whereas the residual is evaluated from the transformed matrices Eqs. (31) and (32):

$$\begin{aligned} \mathbf{R} &= \mathbf{E}^{[2]}(\mathbf{X}) - \omega \mathbf{S}^{[2]}(\mathbf{X}) + \mathbf{B}^{[1]} \\ &= \sum_{i=1}^{2n} (X_{\mathrm{R}})_i (\boldsymbol{\sigma}_i^{2n} - \omega \boldsymbol{\rho}_i^{2n}) + \mathbf{B}^{[1]}. \end{aligned} \tag{38}$$

To accelerate convergence, this residual is preconditioned as

$$\mathbf{M}\ \mathrm{vec}\ \mathbf{R}_{\mathrm{p}} = \mathrm{vec}\ \mathbf{R}, \tag{39}$$

where the preconditioner $\mathbf{M}$ is an easily constructed approximation to $\mathbf{E}^{[2]} - \omega \mathbf{S}^{[2]}$ as discussed in the next section. From the projected preconditioned residual $\mathcal{P}(\mathbf{R}_{\mathrm{p}})$, a new pair of trial matrices $\mathbf{b}_{n+1}$ and $\mathbf{b}_{n+1}^{\mathrm{T}}$ is generated by orthogonalization against the previous basis matrices Eq. (27), ensuring that the new vector pair is normalized and orthogonal,

$$\mathrm{Tr}(\mathbf{b}_{n+1}\mathbf{b}_{n+1}) = 1, \quad \mathrm{Tr}(\mathbf{b}_{n+1}^{\mathrm{T}}\mathbf{b}_{n+1}) = 0, \tag{40}$$

These iterations are continued until the residual is smaller than some preset threshold, using the right-hand side $\mathbf{B}^{[1]}$ of Eq. (7) as an initial guess.

The eigenvalue problem Eq. (19) is solved in the same manner as the response equations, setting up the reduced equations in the space of the $2n$ trial vectors Eq. (27):

$$(\mathbf{E}_{\mathrm{R}}^{[2]} - \omega_{n0}^{\mathrm{R}} \mathbf{S}_{\mathrm{R}}^{[2]})\mathbf{X}_{\mathrm{R},n} = \mathbf{0}. \tag{41}$$

These low-dimensional equations may be solved straightforwardly, yielding an optimal excitation energy $\omega_{n0}^{\mathrm{R}}$ and eigenvector $\mathbf{X}_{\mathrm{R},n}$. The corresponding residual is given by

$$\mathbf{R} = \mathbf{E}^{[2]}(\mathbf{X}_n) - \omega_{n0}^{\mathrm{R}} \mathbf{S}^{[2]}(\mathbf{X}_n), \tag{42}$$

where $\mathbf{X}_n$ is the expansion of the reduced-space eigenvector $\mathbf{X}_{\mathrm{R},n}$ in the trial vectors Eq. (37). This residual may be preconditioned as in Eq. (39) (with $\omega_{n0}^{\mathrm{R}}$ replacing $\omega$ in $\mathbf{M}$) to generate the new pair of trial vectors $\mathbf{b}_{n+1}$ and $\mathbf{b}_{n+1}^{\mathrm{T}}$, and the iterations are continued until convergence. We discuss below how the initial guess of the excitation vector is obtained.

The strategy of adding trial vectors in conjugate pairs (rather than one at a time) not only accelerates the solution by adding two vectors at the cost of one. More importantly, it imposes the correct paired structure on $\mathbf{E}_{\mathrm{R}}^{[2]}$ and $\mathbf{S}_{\mathrm{R}}^{[2]}$, thereby avoiding complex eigenvalues and ensuring monotonic convergence.

## C. Preconditioning

### 1. The AO basis

The preconditioner $\mathbf{M}$ in Eq. (39) should be a good approximation to the response matrix in the sense that the condition number of $\mathbf{M}^{-1}(\mathbf{E}^{[2]} - \omega \mathbf{S}^{[2]})$ should be significantly smaller than that of $\mathbf{E}^{[2]} - \omega \mathbf{S}^{[2]}$. Moreover, the cost of solving the preconditioning equation Eq. (39) should be significantly smaller than that of solving the original response equation Eq. (7). The most expensive step in the solution of Eq. (7) is the evaluation of $\mathbf{G}(\mathbf{D}_{\mathrm{b}})$, which contributes to the two last terms in Eq. (11). Since these terms are small compared with the other terms in Eq. (11), a good preconditioner is given by

$$\mathbf{M} = \mathbf{E}_{\mathrm{F}}^{[2]} - \omega \mathbf{S}^{[2]}, \tag{43}$$

where $\mathbf{E}_{F}^{[2]}$ is an approximation to $\mathbf{E}^{[2]}$ with the last two terms in Eq. (11) neglected:

$$\boldsymbol{\sigma}_{\mathrm{F}} = \mathbf{E}_{\mathrm{F}}^{[2]}(\mathbf{b}) = \mathcal{P}_{\mathrm{T}}(\mathbf{F}\mathbf{D}_{\mathrm{b}}\mathbf{S} - \mathbf{S}\mathbf{D}_{\mathrm{b}}\mathbf{F}). \tag{44}$$

The equations for the preconditioned residual $\mathbf{R}_{\mathrm{p}}$ Eq. (39) may be solved iteratively in the same manner that we solved the response equations Eq. (7).

In solving the response eigenvalue problem Eq. (16), the residual Eq. (42) may be preconditioned as in Eq. (39), using Eq. (43) with $\omega$ replaced by $\omega_{n0}^{\mathrm{R}}$. However, the solution of the preconditioning equation Eq. (39),

$$(\mathbf{E}_{\mathrm{F}}^{[2]} - \omega_{n0}^{\mathrm{R}} \mathbf{S}^{[2]})\mathrm{vec}\ \mathbf{R}_{\mathrm{p}} = \mathrm{vec}\ \mathbf{R}, \tag{45}$$

in the AO basis is difficult since the condition number of $\mathbf{E}_{\mathrm{F}}^{[2]} - \omega_{n0}^{\mathrm{R}} \mathbf{S}^{[2]}$ is large. For a solution to this problem, we examine in the next section the preconditioner in the MO basis.

### 2. The MO basis

An iterative algorithm for solving response eigenvalue and linear equations similar to that presented for the AO basis above has been successfully used in the MO basis,[10,11] where $\mathbf{E}^{[2]}$ and $\mathbf{S}^{[2]}$ are diagonally dominant. In the MO basis, the preconditioner Eq. (43) becomes diagonal,

$$\mathbf{M}_{\mathrm{MO}} = (\mathbf{E}_{\mathrm{F}}^{[2]})_{\mathrm{MO}} - \omega(\mathbf{S}^{[2]})_{\mathrm{MO}} = \begin{pmatrix} \boldsymbol{\Delta\epsilon} & \mathbf{0} \\ \mathbf{0} & \boldsymbol{\Delta\epsilon} \end{pmatrix} - \omega \begin{pmatrix} \mathbf{I} & \mathbf{0} \\ \mathbf{0} & -\mathbf{I} \end{pmatrix}, \tag{46}$$

where the diagonal matrix $\boldsymbol{\Delta\epsilon}$ contains the differences between virtual and occupied orbital energies,

$$\Delta\epsilon_{AI,AI} = \epsilon_A - \epsilon_I. \tag{47}$$

In the MO basis, therefore, the preconditioning may be carried out in a simple manner, dividing the residual $\mathbf{R}$ by the diagonal elements of Eq. (46).

In the AO basis, by contrast, neither $\mathbf{E}_{\mathrm{F}}^{[2]}$ nor $\mathbf{S}^{[2]}$ are diagonally dominant. Furthermore, the condition number of $\mathbf{E}_{\mathrm{F}}^{[2]}$ is significantly larger in the AO basis than in the MO basis, making the iterative solution of Eq. (39) difficult. Since the condition number of a matrix is unaffected by a similarity transformation, we may dramatically improve the conditioning of the equations (reducing the condition number to that of the MO basis) by transforming them to an orthogonal AO basis (OAO) such as the Cholesky basis or the Löwdin basis. Furthermore, in the OAO basis, the preconditioner $\mathbf{M}_{\mathrm{OAO}}$ is much more diagonally dominant than in the original AO basis. In Sec. II C 3, we consider how the preconditioned equations may be solved in the OAO basis. However, we first discuss here how an initial guess of an excitation vector may be obtained.

In the MO basis, the initial guess of an excitation vector has previously been successfully obtained as the solution to the simplified response eigenvalue equations

$$\left[ \begin{pmatrix} \boldsymbol{\Delta\epsilon} & \mathbf{0} \\ \mathbf{0} & \boldsymbol{\Delta\epsilon} \end{pmatrix} - \omega \begin{pmatrix} \mathbf{I} & \mathbf{0} \\ \mathbf{0} & -\mathbf{I} \end{pmatrix} \right] \begin{pmatrix} \mathbf{Y}_{\mathrm{vo}} \\ \mathbf{Y}_{\mathrm{ov}} \end{pmatrix} = \mathbf{0}, \tag{48}$$

where we recognize the simplified response matrix of Eq. (46). In Eq. (48), $\mathbf{Y}_{\mathrm{vo}}$ and $\mathbf{Y}_{\mathrm{ov}}$ are the virtual-occupied and occupied-virtual blocks, respectively, of the matrix

$$\mathbf{Y} = \begin{pmatrix} \mathbf{0} & \mathbf{Y}_{\mathrm{vo}} \\ \mathbf{Y}_{\mathrm{ov}} & \mathbf{0} \end{pmatrix}. \tag{49}$$

The solution of Eq. (48) has zero elements in $\mathbf{Y}_{\mathrm{vo}}$ and $\mathbf{Y}_{\mathrm{ov}}$ except for a unit element in $\mathbf{Y}_{\mathrm{vo}}$ corresponding to the considered orbital-energy difference $\epsilon_A - \epsilon_I$. In Sec. II D, we shall discuss how an equivalent initial vector may be set up in the OAO basis.

#### 3. The orthogonal AO basis

In the OAO basis, the AO overlap matrix is factorized as

$$\mathbf{S} = \mathbf{V}^{\mathrm{T}}\mathbf{V}, \tag{50}$$

where $\mathbf{V}$ is either an upper triangular matrix $\mathbf{U}$ (in the Cholesky basis) or the principal square-root matrix $\mathbf{S}^{1/2}$ (in the Löwdin basis):

$$\mathbf{V}_{\mathrm{C}} = \mathbf{U}, \tag{51}$$

$$\mathbf{V}_{\mathrm{L}} = \mathbf{S}^{1/2}. \tag{52}$$

In Ref. 3, we found that both schemes give diagonally dominant Hessians, with a slight preference for the Löwdin basis. An advantage of the Löwdin basis is that, among all possible orthogonal bases, it resembles most closely the original AO basis, ensuring that locality is preserved to the greatest possible extent. Furthermore, the transformation to the Löwdin basis can be performed straightforwardly within a linear-scaling framework.[22] Except as noted, we use the Löwdin basis in our calculations.

In the OAO basis defined by Eq. (50), the linear transformations entering Eq. (39) become

$$(\boldsymbol{\sigma}_{\mathrm{F}})_{\mathrm{V}} = (\mathbf{F}_{\mathrm{V}}^{\mathrm{vv}} - \mathbf{F}_{\mathrm{V}}^{\mathrm{oo}})\mathbf{X}^{\mathrm{V}} + \mathbf{X}^{\mathrm{V}}(\mathbf{F}_{\mathrm{V}}^{\mathrm{vv}} - \mathbf{F}_{\mathrm{V}}^{\mathrm{oo}}), \tag{53}$$

$$\boldsymbol{\rho}_{\mathrm{V}} = \mathbf{D}^{\mathrm{V}}\mathbf{X}^{\mathrm{V}} - \mathbf{X}^{\mathrm{V}}\mathbf{D}^{\mathrm{V}}, \tag{54}$$

where we have used the notations

$$\mathbf{A}_{\mathrm{V}} = \mathbf{V}^{-\mathrm{T}}\mathbf{A}\mathbf{V}^{-1}, \tag{55}$$

$$\mathbf{A}^{\mathrm{V}} = \mathbf{V}\mathbf{A}\mathbf{V}^{\mathrm{T}}. \tag{56}$$

The preconditioning of the residual for the response equations Eq. (39) is performed in the OAO basis and the conjugate-gradient algorithm may be used with the diagonal preconditioner

$$M_{\alpha\beta,\alpha\beta} = (\mathbf{F}_{\mathrm{V}}^{\mathrm{vv}} - \mathbf{F}_{\mathrm{V}}^{\mathrm{oo}})_{\alpha\alpha} + (\mathbf{F}_{\mathrm{V}}^{\mathrm{vv}} - \mathbf{F}_{\mathrm{V}}^{\mathrm{oo}})_{\beta\beta} - \omega[(\mathbf{D}^{\mathrm{V}})_{\alpha\alpha} - (\mathbf{D}^{\mathrm{V}})_{\beta\beta}]. \tag{57}$$

The preconditioning of the residual of the eigenvalue equations may be carried out in the same manner but with the frequency $\omega$ replaced by the excitation energy $\omega_{n0}^{\mathrm{R}}$.

### D. Initial vectors for the response eigenvalue equation

In the MO basis, the $\mathbf{Y}$ matrix in Eq. (49) has been successfully used to obtain an initial guess of the excitation vector in the iterative solution of the response eigenvalue equations. The $\mathbf{Y}$ matrix is zero except for a unit element $Y_{AI}$ corresponding to the considered orbital-energy difference $\epsilon_A - \epsilon_I$. If the lowest excitation energy is determined, the lowest orbital energy difference [i.e., the highest occupied molecular orbital (HOMO)–lowest unoccupied molecular orbital (LUMO) gap] is considered and similarly for higher excited states. In the OAO basis of Eq. (50), the initial vector becomes

$$\mathbf{Y}_{\mathrm{OAO}} = \mathbf{C}\mathbf{Y}_{\mathrm{MO}}\mathbf{C}^{\mathrm{T}}, \tag{58}$$

where $\mathbf{C}$ contains the eigenvectors of the Fock/KS matrix in the OAO basis,

$$\mathbf{F}_{\mathrm{V}}\mathbf{C} = \boldsymbol{\epsilon}\mathbf{C}. \tag{59}$$

For an initial guess that is represented by a unit element $Y_{AI}$ in the MO basis, the OAO initial vector becomes

$$(\mathbf{Y}_{\mathrm{OAO}})_{\mu\nu} = C_{\mu A}C_{\nu I}, \tag{60}$$

where indices $\mu$ and $\nu$ refer to OAO basis. In this basis, the projectors onto the occupied and virtual spaces become

$$\mathbf{P}_{\mathrm{o}}^{\mathrm{OAO}} = \mathbf{D}^{\mathrm{V}}, \tag{61}$$

$$\mathbf{P}_{\mathrm{v}}^{\mathrm{OAO}} = \mathbf{1} - \mathbf{D}^{\mathrm{V}}. \tag{62}$$

The Fock/KS eigenvalue equation in Eq. (59) may then be written as

$$(\mathbf{P}_o^{OAO}\mathbf{F}_V\mathbf{P}_o^{OAO} + \mathbf{P}_v^{OAO}\mathbf{F}_V\mathbf{P}_v^{OAO})\mathbf{C} = \boldsymbol{\epsilon}\mathbf{C}, \quad (63)$$

since $\mathbf{P}_o^{OAO}\mathbf{F}_V\mathbf{P}_v^{OAO} = \mathbf{P}_v^{OAO}\mathbf{F}_V\mathbf{P}_o^{OAO} = \mathbf{0}$ for an optimized state. Projecting Eq. (63) onto the occupied and virtual spaces, we obtain

$$\mathbf{P}_o^{OAO}\mathbf{F}_V\mathbf{P}_o^{OAO}\mathbf{C} = \boldsymbol{\epsilon}\mathbf{P}_o^{OAO}\mathbf{C}, \quad (64)$$

$$\mathbf{P}_v^{OAO}\mathbf{F}_V\mathbf{P}_v^{OAO}\mathbf{C} = \boldsymbol{\epsilon}\mathbf{P}_v^{OAO}\mathbf{C}, \quad (65)$$

demonstrating that the orbital energies and eigenvectors of the occupied and virtual spaces can be obtained from Eqs. (64) and (65), respectively. Using iterative techniques, we may thus determine the eigenvectors of the highest occupied orbitals from Eq. (64) and of the lowest virtual orbitals from Eq. (65). Subsequently, Eq. (60) may be used to generate start vectors in the OAO basis.

## III. ILLUSTRATIVE RESULTS

In this subsection, we report calculations of excitation energies and frequency-dependent polarizabilities for polyalanine peptides of increasing size. The polyalanines are one-dimensional systems and thus ideal systems for demonstrating that linear scaling is approached. The largest peptide contains 139 alanine residues and 1392 atoms. We use CAM-B3LYP/6-31G to calculate the lowest excitation energy and Hartree-Fock/6-31G to calculate the frequency-dependent polarizability at a frequency of 0.1 a.u. The CAM-B3LYP (Ref. 23) functional is chosen because it gives significantly improved molecular properties compared with the B3LYP functional.[24] For each type of property calculation, we analyze both the scaling with respect to increasing molecular size and the convergence characteristics of the algorithm on one selected peptide—namely, ALA119 (containing 119 alanine residues) for the frequency-dependent polarizability and ALA59 for the excitation energy calculation. The SCF convergence is similar to that described for the ALA99 calculations in Ref. 3. All calculations have been carried out using a local version of DALTON.[25] The timings are obtained using a single processor on a SUN Fire X4600 (Opteron, 2.6 GHz).

### A. The frequency-dependent polarizability of a peptide with 119 alanine residues

In this section, we describe a typical frequency-dependent polarizability calculation using ALA119 as an example. First, the response equations Eq. (7) are solved at a frequency of 0.1 a.u., after which the polarizability is obtained as the trace of the property gradient and the solution matrix according to Eq. (6). The linear equations are solved in the AO basis, using the iterative algorithm of Sec. II B. At each iteration, the residual is transformed to the Löwdin basis and preconditioned as described in Sec. II C. As initial trial vector for the response equations, the property gradient is used.

In Table I, we have listed the residual at each iteration in the solution of the linear equations Eq. (7). Convergence to a Frobenius norm of $10^{-2}$ of the residual is obtained in ten iterations. At each linear-response iteration, the residual is preconditioned by solving the linear equations Eq. (39) with $\mathbf{M}$ given in Eq. (43) in the Löwdin basis, using the linear transformations Eqs. (53) and (54) and the diagonal preconditioner Eq. (57). The iterations are terminated when the residual of Eq. (39) (in the Löwdin basis) has been reduced by a factor of 100 (the overall convergence of the response equations is not sensitive to the choice of this threshold.) As seen from Table I, for all response iterations, the preconditioning equations converge in seven iterations, which is the case in all polarizability calculations presented here.

TABLE I. The residual norm $\|\mathbf{R}\|$ and the number of preconditioning iterations $n_{pre}$ for the calculation of the frequency-dependent polarizability at $\omega$=0.1 a.u. of ALA119 at the Hartree-Fock/6-31G level of theory.

| It. | $\|\mathbf{R}\|$ | $n_{pre}$ |
|---|---|---|
| 1 | 28.10 | 7 |
| 2 | 12.71 | 7 |
| 3 | 3.967 | 7 |
| 4 | 1.776 | 7 |
| 5 | 0.746 | 7 |
| 6 | 0.326 | 7 |
| 7 | 0.125 | 7 |
| 8 | 0.060 | 7 |
| 9 | 0.027 | 7 |
| 10 | 0.011 | 7 |

We now consider in more detail the preconditioning of the first trial vector of the ALA119 calculation. In Table II, we have listed the residual of the preconditioning equations Eq. (39), with and without the diagonal preconditioner Eq. (57). Although the diagonal preconditioner dramatically improves convergence, its use requires that the trial vectors are projected, since the preconditioning introduces redundant components. The projection requires four additional matrix

TABLE II. Convergence of the preconditioning equations in the first response iteration of the Hartree-Fock/6-31G calculation of the frequency-dependent polarizability $\omega$=0.1 a.u. of ALA119. The residual norms are given in the Löwdin and Cholesky bases, with and without diagonal preconditioning.

| | Löwdin basis | | Cholesky basis | |
|---|---|---|---|---|
| It. | No. prec. | Dia. prec. | No. prec. | Dia. prec. |
| 1 | 82.20 | 82.20 | 82.20 | 82.20 |
| 2 | 42.15 | 19.39 | 41.94 | 19.27 |
| 3 | 41.16 | 7.36 | 41.12 | 9.11 |
| 4 | 27.82 | 5.04 | 27.96 | 5.56 |
| 5 | 13.47 | 2.26 | 13.19 | 2.68 |
| 6 | 18.05 | 0.98 | 18.05 | 1.24 |
| 7 | 8.44 | 0.43 | 8.41 | 0.59 |
| 8 | 6.59 | | 6.61 | |
| 9 | 7.18 | | 7.16 | |
| 10 | 3.87 | | 3.88 | |
| 11 | 2.90 | | 2.89 | |
| 12 | 2.19 | | 2.19 | |
| 13 | 1.48 | | 1.48 | |
| 14 | 1.29 | | 1.29 | |
| 15 | 0.82 | | 0.81 | |
| 16 | 0.56 | | | |

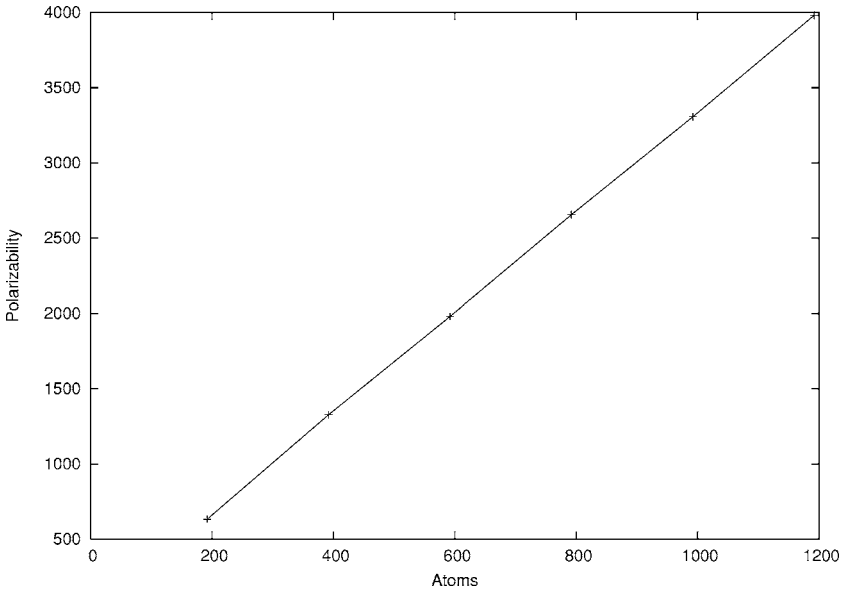


FIG. 1. The $xx$ component of the Hartree-Fock/6-31G frequency-dependent dipole polarizability ($\omega$ =0.1 a.u.) for polyalanines (atomic units).

multiplications per iteration, making preconditioning less attractive. We nevertheless recommend its use since otherwise the equations sometimes do not converge.

We use the Löwdin OAO basis by default but have also included in Table II information about convergence in the Cholesky basis. Although the Löwdin basis sometimes gives faster convergence than the Cholesky basis, the situation illustrated in Table II is fairly typical, with a nearly identical behavior in the two bases.

The convergence of the response equations reported here is typical of polarizability calculations and similar to that of the standard MO-based iterative algorithm of Ref. 11 [implemented in DALTON (Ref. 25)]. Any difference in convergence arises because the preconditioning equations are terminated when the residual has been reduced by a factor of 100. If the preconditioning equations were converged to full accuracy, identical results would be obtained in the AO and MO bases.

### B. Linear-scaling frequency-dependent polarizability calculations

In Fig. 1, the frequency-dependent dipole longitudinal polarizability $\alpha_{xx}(\omega)$ at $\omega$=0.1 a.u. is plotted as a function of the number of atoms in polyalanine peptides, calculated at the Hartree-Fock/6-31G level of theory. As expected, the longitudinal polarizability depends linearly on the number of atoms. In Fig. 2, we have plotted the CPU times of the different parts of the polarizability calculations, using the block sparse-matrix scheme described by Rubensson and Sałek in Ref. 26. The timings are for the following contributions in the first response iteration: the Coulomb part ("Fock J") and the exchange part ("Fock X") of the $\mathbf{G}(\mathbf{D}_b)$ contribution to the linear transformation Eq. (11), the remainder of the linear transformations Eqs. (11) and (12) ("Lintra"), and the preconditioning of the trial vectors ("Precond").

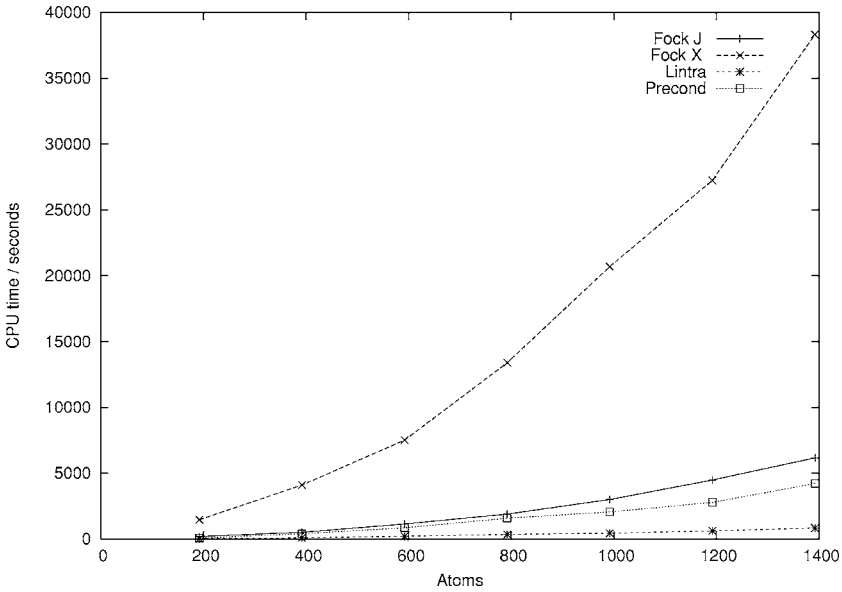


FIG. 2. Timings for the different parts of a Hartree-Fock/6-31G response iteration in a frequency-dependent polarizability calculation ($\omega$=0.1 a.u.) for polyalanines. Sparse-matrix algebra is used.

TABLE III. The residual norm $\|\mathbf{R}\| \times 10^3$ and the number of preconditioning iterations $n_{\text{pre}}$ for the calculation of the lowest excitation energy of ALA59 at the CAM-B3LYP/6-31G level of theory (full-matrix algebra).

| It. | $\|\mathbf{R}\| \times 10^3$ | $n_{\text{pre}}$ |
|---|---|---|
| 1 | 0.197 | 20 |
| 2 | 0.057 | 20 |
| 3 | 0.066 | 20 |
| 4 | 0.014 | 20 |
| 5 | 0.008 | 20 |

The Hartree-Fock polarizability calculations are dominated by the exchange contribution to the linear transformation, whose calculation approaches linearity for systems containing more than 600 atoms. The Coulomb evaluation (by density fitting) is several times faster than the exchange evaluation. For the remaining two contributions in Fig. 2, the time-consuming parts consist of matrix multiplications and scale linearly with system size, showing that matrix sparsity is efficiently exploited in our calculations.

### C. The lowest excitation energy for a peptide with 59 alanine residues

In this section, we consider the calculation of excitation energies for large systems using ALA59 in full-matrix algebra as an example. Excitation energies are eigenvalues of the response eigenvalue problem Eq. (19), which is solved in the AO basis using the iterative algorithm of Sec. II B. At each iteration, the residual is transformed to the Löwdin basis and preconditioned as described in Sec. II C. As an initial eigenvector guess, we use Eq. (60), where the eigenvectors of the Fock/KS matrix in the occupied and virtual spaces are determined from Eqs. (64) and (65), respectively.

In Table III, we have listed the residual at each iteration of the solution of the response eigenvalue problem Eq. (19). The response iterations are terminated when the residual norm has been reduced by a factor of 100, which is obtained in five iterations. At each iteration, the residual is preconditioned by solving the simplified response equations Eq. (45) in the Löwdin basis, using the linear transformations of Eqs. (53) and (54) and the diagonal preconditioner Eq. (57). The preconditioning iterations are also terminated when the residual of Eq. (45) (in the Löwdin basis) has been reduced by a factor of 100 or after a maximum of 20 iterations. As indicated in Table III, the preconditioning equations always terminated at the maximum number of iterations, which is true for all excitation energy calculations presented here.

We now consider in more detail the preconditioning of the first trial vector of the ALA59 calculation. Full-matrix rather than sparse-matrix algebra was used in this calculation, since the residual is very small already in the first response iteration, and the efficiency of the preconditioner becomes blurred by numerical noise when sparse-matrix algebra is used. In Table IV, we have listed the residual of the preconditioning equations Eq. (45), with and without the diagonal preconditioner Eq. (57). Without preconditioning, the equations do not converge. With preconditioning, the residual decreases slowly until, after the maximum number of allowed iterations, it has been reduced by about an order of magnitude. Clearly, it is much more difficult to converge the preconditioning equations for the response eigenvalue equations than for the response linear equations.

TABLE IV. Convergence of the preconditioning equations in the first response iteration of the CAM-B3LYP/6-31G calculation of the lowest excitation energy of ALA59 (full-matrix algebra). The residual norms are given with and without diagonal preconditioning

| | $\|\mathbf{R}\| \times 10^3$ | |
|---|---|---|
| It. | No prec. | Dia. prec. |
| 1 | 0.309 | 0.309 |
| 2 | 0.364 | 0.253 |
| 3 | 0.235 | 0.349 |
| 4 | 0.413 | 0.303 |
| 5 | 0.368 | 0.262 |
| 6 | 0.276 | 0.249 |
| 7 | 0.429 | 0.201 |
| 8 | 0.272 | 0.161 |
| 9 | 0.335 | 0.135 |
| 10 | 0.321 | 0.135 |
| 11 | 0.230 | 0.122 |
| 12 | 0.370 | 0.122 |
| 13 | 0.258 | 0.118 |
| 14 | 0.241 | 0.107 |
| 15 | 0.368 | 0.091 |
| 16 | 0.201 | 0.073 |
| 17 | 0.230 | 0.060 |
| 18 | 0.226 | 0.047 |
| 19 | 0.153 | 0.042 |

To understand this difference between the response linear and eigenvalue equations, consider the carrier matrix Eq. (43) for the preconditioning equations $\mathbf{E}_{\text{F}}^{[2]} - \omega\mathbf{S}^{[2]}$, where $\omega$ is either the frequency of the applied field (linear equations) or a reduced-space eigenvalue (eigenvalue equations). The approximate generalized electronic Hessian $\mathbf{E}_{\text{F}}^{[2]}$ is positive definite provided the optimized Hartree-Fock or Kohn-Sham energy is a minimum—it is a well-behaved matrix that (when preconditioned) has a relatively small condition number. Consequently, rapid convergence is observed when the linear equations are solved in the static limit; moreover, since the applied frequency is typically small (0.1 a.u. in Sec. III A), the addition of $-\omega\mathbf{S}^{[2]}$ to $\mathbf{E}_{\text{F}}^{[2]}$ does not affect the convergence of the linear equations.

By contrast, in the solution of the response eigenvalue problem, the addition of $\omega_{n0}^{\text{R}}\mathbf{S}^{[2]}$ changes the structure of the carrier matrix, making $\mathbf{E}_{\text{F}}^{[2]} - \omega_{n0}^{\text{R}}\mathbf{S}^{[2]}$ nearly singular and ill conditioned. As a result, the preconditioning equations are much more difficult to converge for the response eigenvalue equations than for the linear equations. However, as seen from Table III, the eigenvalue equations can nevertheless be converged in a few iterations, because of the good starting guess of Eq. (60). When the Cholesky rather than the Löwdin basis is used for the preconditioning equations, the convergence is similar to that in the Löwdin basis.

### D. Linear-scaling calculations of excitation energies

In Fig. 3, the lowest excitation energy, the lowest Hessian eigenvalue, and the HOMO-LUMO gap are plotted as

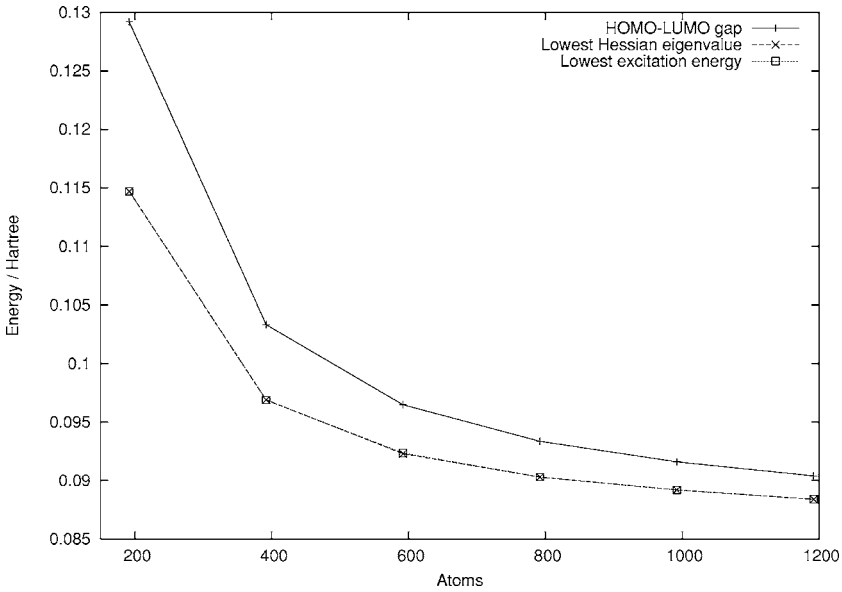


FIG. 3. The HOMO-LUMO gap, the lowest Hessian eigenvalue, and the lowest excitation energy for polyalanines, calculated at the CAM-B3LYP/6-31G level of theory.

functions of the number of atoms in polyalanine peptides at the CAM-B3LYP/6-31G level of theory. As expected, the excitation energy decreases with increasing system size. More surprisingly, the lowest Hessian eigenvalue and the lowest excitation energy are equal to the number of significant digits. To understand this behavior, consider the evaluation of excitation energies in the MO basis, where the response eigenvalue equation in a notation similar to that of Eq. (48) becomes

$$\left[\begin{pmatrix}\mathbf{A} & \mathbf{B}\\ \mathbf{B} & \mathbf{A}\end{pmatrix} - \omega\begin{pmatrix}\mathbf{I} & \mathbf{0}\\ \mathbf{0} & -\mathbf{I}\end{pmatrix}\right]\begin{pmatrix}\mathbf{Y}_{\mathrm{vo}}\\ \mathbf{Y}_{\mathrm{ov}}\end{pmatrix} = \mathbf{0}. \tag{66}$$

The **B** matrix contains Hamiltonian matrix elements between the Kohn-Sham determinant and a doubly excited configuration. If it vanishes, the eigenvalues $\omega$ of Eq. (66) become equal to the eigenvalues of the electronic Hessian $\mathbf{A}-\mathbf{B}$. The exact exchange in CAM-B3LYP gives a nonzero **B** matrix contribution but is too small to be detected. The HOMO-LUMO gap is slightly above the calculated excitation energies, as expected from the form of the **A** matrix, which contains the orbital-energy difference of Eq. (48) with Coulomb and exchange-correlation contributions subtracted.

In Fig. 4, we have plotted the CPU times of excitation-energy calculations when sparse-matrix algebra is used, for the following contributions to the first response iteration: the Coulomb contribution to the linear transformation Eq. (11) ("Kohn-Sham J"), the exact-exchange contribution ("Kohn-Sham X"), the exchange-correlation contribution ("Kohn-Sham XC"), the remainder of the linear transformations Eqs. (11) and (12) ("Lintra"), and the preconditioning of the trial vectors ("Precond").

The excitation energy calculations are dominated by the exchange-correlation contribution. Comparing with the Hartree-Fock polarizability calculations in Fig. 2, we note that the evaluation of the Coulomb and exact-exchange contributions is much faster in the Kohn-Sham excitation energy calculations in Fig. 4. The difference arises since the timings are given for the first response iteration, for which the start-

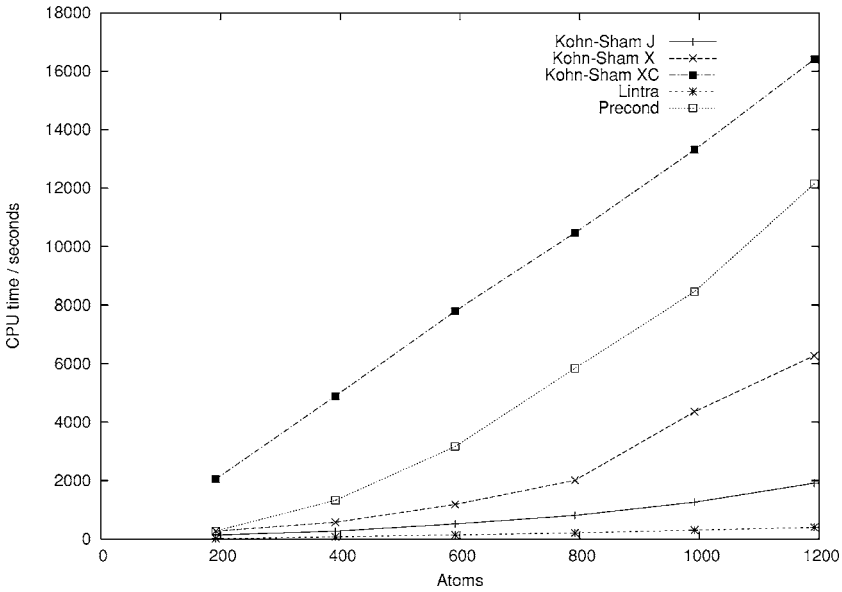


FIG. 4. Timings for different parts of a response iteration in a CAM-B3LYP/6-31G excitation energy calculation for polyalanines. Sparse-matrix algebra is used.

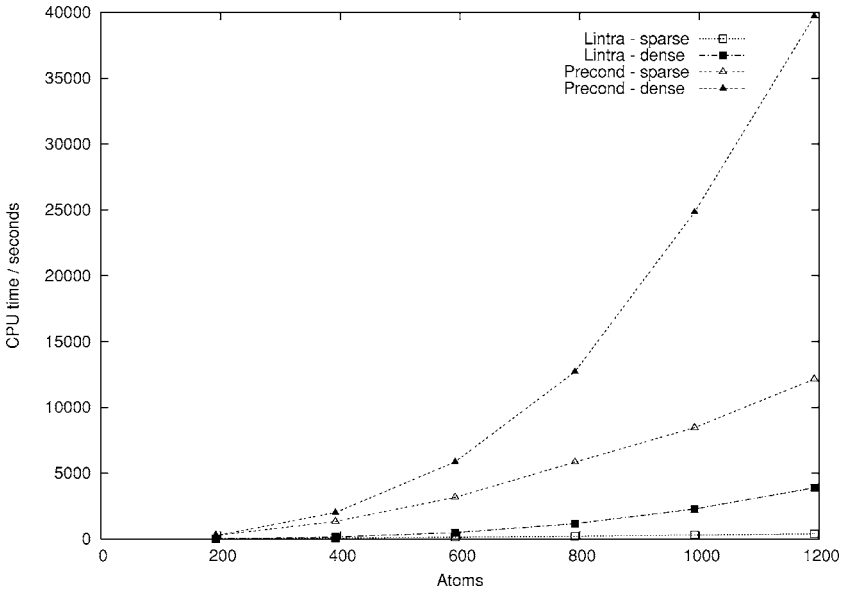


FIG. 5. Comparison of sparse- and dense-matrix timings for selected parts of a CAM-B3LYP/6-31G response iteration in an excitation energy calculation for polyalanines.

ing guess for excitation energies is more sparse than the one for polarizabilities. Also, preconditioning is more expensive for excitation energies than for polarizabilities since about three times more iterations are needed. As a result, preconditioning becomes more expensive than the evaluation of the Coulomb and exact-exchange contributions.

As seen from Fig. 4, the cost of the exchange-correlation contribution to the linear transformation scales linearly with system size. The same is true for the Coulomb contribution, while the evaluation of exact exchange is nonlinear, at least for small systems. For the Lintra and Precond contributions to the response equations, the time-consuming parts consist of matrix-matrix multiplications. The scaling of these contributions shows that sparsity is efficiently exploited, although the Precond contribution shows signs of nonlinear scaling. Investigation of the time spent in the preconditioning shows that the matrices involved in the linear transformation have not yet reached the regime of linear scaling in the number of nonzero elements. The benefits of sparse-matrix algebra are nevertheless evident from Fig. 5, where we compare the Lintra and Precond timings of Fig. 4 with those obtained using full-matrix algebra. Whereas the cost increases cubically when full-matrix algebra is used, linear scaling is approached with sparse-matrix algebra.

## IV. CONCLUSIONS

Using the nonredundant exponential parametrization of the density matrix introduced in Refs. 1 and 18, we have presented a linear-scaling implementation of excitation energies and frequency-dependent second-order molecular properties. The response eigenvalue and linear equations are solved using an iterative subspace method equivalent to the one that has been successfully used in the MO basis. Important features of the subspace method are the use of paired trial vectors (to preserve the structure of the full equations in the reduced space), a nondiagonal preconditioning (for rapid convergence), and good start vectors (for robust and fast solution). The performance is similar to that in the MO basis, with five to ten iterations needed for convergence. The preconditioning is carried out in the Löwdin basis, solving a simplified version of the response equations with an iterative method similar to the one used for the full response equations. To reduce the residual of the preconditioning equations by a factor of 100, less than ten iterations are typically needed for the response linear equations. For the response eigenvalue equations, the preconditioning equations are more difficult to converge, easily requiring 20 iterations.

As for the optimization of the Hartree-Fock and KS density matrices, the solution of the response equations is dominated by the construction of the Fock/KS matrix, once at each iteration of the subspace algorithm. The solution of the preconditioning equations is dominated by matrix-matrix multiplications, for which linear scaling is approached by using sparse-matrix algebra. Calculations of the frequency-dependent polarizability at $\omega=0.1$ a.u. and of the lowest excitation energy have been presented for polyalanine peptides containing up to 1400 atoms, demonstrating the efficiency and robustness of the presented algorithm and that linear scaling can be obtained in such calculations.

## ACKNOWLEDGMENTS

This work has been supported by the Lundbeck Foundation, the Danish Natural Research Council, and the Norwegian Research Council through a Strategic University Program in Quantum Chemistry (Grant No. 154011/420) and through a grant of computer time from the Program for Supercomputing. The authors also acknowledge support from the Danish Center for Scientific Computing (DCSC) and the European Research and Training Network "NANOQUANT, Understanding Nanomaterials from the Quantum Perspective," Contract No. MRTN-CT-2003-506842. One of the authors (S.C.) acknowledges support from the Italian Consiglio Nazionale delle Ricerche through a Short Term Mobility Grant.

[1] T. Helgaker, P. Jørgensen, and J. Olsen, *Molecular Electronic-Structure Theory* (Wiley, Chichester, 2000).
[2] *Advances in Quantum Chemistry 50 - Response Theory and Molecular Properties (A Tribute to Jan Linderberg and Poul Jørgensen)*, edited by

H. J. Aa. Jensen (Elsevier, New York, 2005).
[3] P. Sałek, S. Høst, L. Thøgersen *et al.*, J. Chem. Phys. **126**, 114110 (2007).
[4] S. Goedecker and G. E. Scuseria, Comput. Sci. Eng. **5**, 14 (2003).
[5] S. Goedecker, Rev. Mod. Phys. **71**, 1085 (1999).
[6] J. Olsen and P. Jørgensen, J. Chem. Phys. **82**, 3235 (1985).
[7] H. Larsen, P. Jørgensen, J. Olsen, and T. Helgaker, J. Chem. Phys. **113**, 8908 (2000).
[8] J. Olsen (unpublished).
[9] L. Thøgersen, Ph.D. thesis, Aarhus University, 2005.
[10] J. Olsen and P. Jørgensen, in *Modern Electronic Structure Theory*, edited by D. R. Yarkony (World Scientific, Singapore, 1995), pt. II.
[11] J. Olsen, H. J. A. Jensen, and P. Jørgensen, J. Comput. Phys. **74**, 265 (1988).
[12] Y. Shao, C. Saravanan, M. Head-Gordon, and C. A. White, J. Chem. Phys. **118**, 6144 (2003).
[13] C. Ochsenfeld and M. Head-Gordon, Chem. Phys. Lett. **270**, 399 (1997).
[14] R. McWeeny, Rev. Mod. Phys. **32**, 325 (1960).
[15] X. P. Li, R. W. Nunes, and D. Vanderbilt, Phys. Rev. B **47**, 10891 (1993).
[16] C. Ochsenfeld, J. Kussmann, and F. Koziol, Angew. Chem., Int. Ed. **43**, 4485 (2004).
[17] V. Weber, A. M. N. Niklasson, and M. Challacombe, J. Chem. Phys. **123**, 044107 (2005).
[18] T. Helgaker, H. Larsen, J. Olsen, and P. Jørgensen, Chem. Phys. Lett. **327**, 397 (2000).
[19] H. Larsen, J. Olsen, P. Jørgensen, and T. Helgaker, J. Chem. Phys. **115**, 9685 (2001).
[20] H. Larsen, T. Helgaker, P. Jørgensen, and J. Olsen, J. Chem. Phys. **115**, 10344 (2001).
[21] H. Larsen, Ph.D. thesis, Aarhus University, 2001.
[22] B. Jansík, S. Høst, P. Jørgensen, and T. Helgaker, J. Chem. Phys. **126**, 124104 (2007).
[23] T. Yanai, D. P. Tew, and N. C. Handy, Chem. Phys. Lett. **393**, 51 (2004).
[24] M. J. G. Peach, T. Helgaker, P. Sałek, T. W. Keal, O. B. Lutnæs, D. J. Tozer, and N. C. Handy, Phys. Chem. Chem. Phys. **558**, 8 (2006).
[25] DALTON, an *ab initio* electronic structure program, Release 2.0, 2005 (see http://www.kjemi.uio.no/software/dalton/dalton.html).
[26] E. H. Rubensson and P. Sałek, J. Comput. Chem. **26**, 1628 (2005).